Integration of ultrasonic transducers in fast prototyping microfluidic devices

S. S. Guo,[1,a)] S. T. Lau,[2] K. H. Lam,[2] Y. L. Deng,[3] X. Z. Zhao,[3] Y. Chen,[4] and H. L. W. Chan[2]

[1]*Department of Applied Physics, The Hong Kong Polytechnic University, Hung Hom, Kowloon, Hong Kong, People's Republic of China and Department of Physics, Key Laboratory of Acoustic and Photonic Materials and Devices of Ministry of Education, Wuhan University, Wuhan, Hubei 430072, People's Republic of China*

[2]*Department of Applied Physics, The Hong Kong Polytechnic University, Hung Hom, Kowloon, Hong Kong, People's Republic of China*

[3]*Department of Physics, Key Laboratory of Acoustic and Photonic Materials and Devices of Ministry of Education, Wuhan University, Wuhan, Hubei 430072, People's Republic of China*

[4]*Department of Applied Physics, The Hong Kong Polytechnic University, Hung Hom, Kowloon, Hong Kong, People's Republic of China and Ecole Normale Supérieure of Paris, 24 rue Lhomond, 75005 Paris, France*

(Received 20 December 2007; accepted 27 February 2008; published online 5 May 2008)

Bulk acoustic wave induced mixing in microfluidic systems has been studied by using a pair of small size ultrasonic transducers integrated into a prototype polydimethylsiloxane device. The acoustic properties of the integrated ultrasonic transducers were evaluated, demonstrating the generation of bulk acoustic wave in the mixing chamber when a low ac voltage is applied. Then, the mixing efficiency of the device was studied by using two stream laminar flows and taking into account the particular geometry of the mixing chamber. Because of the limited power consumption, the system should be compatible with the requirements of a number of applications in both analytical chemistry and biology. © *2008 American Institute of Physics*. [DOI: 10.1063/1.2912825]

I. INTRODUCTION

Active mixing of chemical solutions is often required to improve the reaction efficiency at the microscale, which is of great importance for the development of a variety of advanced applications in analytical chemistry and in biology, including clinical diagnosis, drug delivery, and biochemical synthesis.[1–6] Previously, a large number of mixing mechanisms and devices were proposed based on both microelectromechanical system and micrototal-analysis-system techniques.[7–10] In most cases, external energy is introduced into the mixer in which two fluidic streams flow, and the mixing performance can be improved by periodic vibration or chaotic advection of the flow fields.

There are many fluid actuation methods, including surface acoustic wave (SAW),[11] time pulsing,[12] and electrowetting-based droplets.[13] Moroney *et al.*[14] investigated the acoustic streaming effect generated by ultrasonic actuation whereby the flow field produces instability to effectively promote the mixing of fluids. Tseng *et al.*[11] reported a SAW technique with interdigitized transducers for protein-enzyme mixing in the megahertz frequency range. However, the mixing efficiency is dramatically affected when such SAW passes through fluidic media, as fluids do not support shear waves, leading to severe attenuation at high frequencies.

Mixing with bulk acoustic wave (BAW) has also attracted considerable attention during the last decades[15–18] due to their unique advantages such as higher energy output, nondestructive detection, and easy manipulation. A properly controlled sound field can be used for breaking up agglomeration, separation, trapping, and deformation of small particles as well as biological objects. Among various BAW techniques, piezoelectric element-generated ultrasonic vibration has proven to be a powerful tool for microfluidic applications. Yang *et al.* reported an active micromixer that used ultrasonic vibration (48 kHz) through an oscillating diaphragm structure activated by piezoelectric lead-zirconate-titanate (PZT) ceramic.[19] Liu *et al.* also developed a mixer that consisted of a piezoelectric disk based on the principle of bubble-induced acoustic microstreaming, which set air bubbles vibrating in circulatory flows with rapid mixing.[20] Their devices were fabricated on glass and silicon substrates by using etching and anodically bonding processes, which were combined with photolithography techniques.

Though the targeting flows were intensively mixed by BAW techniques, a rise in temperature was found due to the low-frequency (in kilohertz) ultrasonic irradiation. It is an inevitable drawback existing in such devices for biological applications. Besides, effective mixing is challenging due to their low Reynolds number of flow conditions inherent in these laminar systems. Hence, developing techniques to enhance the diffusion-dominated mixing process within microfluidic devices has become a crucial issue. Much work needs to be done to optimize the design in order to improve the efficiency of acoustic mixing in microfluidic systems.

In our work, we demonstrate a simple way through using BAW, instead of complex geometries and expensive procedures. The integrated microfluidic device was developed for versatile mixing employing a two-layer polydimethylsilox-

[a)]Electronic mail: gssyhx@whu.edu.cn.

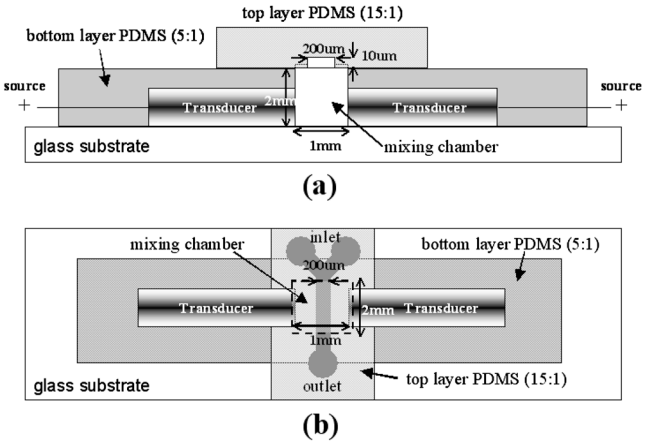

FIG. 1. (Color online) Schematic of a integrated microfluidic device using a pair of ultrasonic transducers. (a) Cross section of the integrated chip and (b) overview of the chip with two-layer PDMS structure. The PDMS channel of the top layer is 200 μm wide and 10 μm deep. The mixing chamber is 1 mm wide, 2 mm deep, and 2 mm long. The size markers just illustrate the design without corresponding to a real ratio of dimensions.

ane (PDMS) units by using a soft-photolithographic technique. Effective ultrasonic forces were induced by a pair of piezoelectric transducers located on the bottom of the mixing chamber. A fast and efficient mixing was implemented when tested by laminar flows, particles of Fe_3O_4 colloid, and proliferation of yeast cells. The device has limited power consumptions without an obvious Joule heating effect and is particularly attractive for bioassay.

II. MATERIALS AND METHODS

A. Materials and chemicals

A commercial PDMS kit (RTV 615) was purchased from GE Toshiba Silicones Co. Ltd. A photoresist (AZ 50XT) and a developer were obtained from Clariant Corp. Silicon wafers were purchased from Luoyang Single Crystal Silicon Co., China. Other chemicals were obtained from the Centre for Smart Materials of the Hong Kong Polytechnic University. The oil phase used here was soybean oil (0.92 g/cm^3). A solution of Fe_3O_4 colloid was synthesized by a codeposition method and yeast cells were obtained from CCTCC (China Centre for Typical Culture Collection). All of the solutions were prepared with ultrapure water (18.2 MΩ cm) from a Simplicity 185 pure water system (Millipore, USA). The active elements of ultrasonic transducers were piezoelectric ceramic pieces ($0.5\times0.5\times0.48$ mm^3) that used $Pb(Zr,Ti)O_3$ based compositions (PZT 5H from PKI, USA) with a relatively high d_{33} piezoelectric coefficient.

B. Configuration of the ultrasonic-transducer-integrated microfluidic device

Figure 1 shows a schematic of the microfluidic device designed and realized in this work, which consisted of a two-layer PDMS structure with two integrated ultrasonic transducers. Its fabrication process is as follows: The glass substrates were cleaned by trichloroethylene, acetone, isopropanol, and de-ionized water in sequence. First, the bottom layer of PDMS was spin coated on a cleaned glass substrate with a 5:1 ratio (prepolymer and crosslinking polymer) mixture. Then, a pair of piezoelectric transducers was assembled along the axial direction immersed into the PDMS on glass substrate. The distance between the two planar faces of transducers was set as 1 mm [Fig. 1(a)]. After being leveled on a stable stage, the PDMS containing the transducers was cured at 80 °C for 2 h. Second, the mold of the upper channel was defined by using replica molding through soft photolithography. The photoresist (AZ 50XT) was spin coated on a silicon wafer and then patterned with a high precision transparency mask. After development, trimethylchlorosilane was evaporated on the photoresist master. A 15:1 ratio of PDMS mixture was poured on and cured with a typical channel height of 10 μm. Finally, the two PDMS layers were sealed through oxygen plasma treatment (PDC-32G, Harrick Plasma, USA) with a microscopy aligner and cured at 80 °C for 4 h. A mixing chamber was formed with dimensions of $2\times2\times1$ mm^3 [Fig. 1(b)]. After assembling, the microfluidic chip was placed on the sample stage of an inverted fluorescence microscope (Olympus X71) equipped with a monochrome cooled charge-coupled device camera (Model 32-0105B-146, Evolution™ VF) for the image capture. The micrographs were analyzed by commercial software IPP (Imaging Pro Plus 5.1, Media Cybernetics, Inc.).

C. Fabrication of ultrasonic transducers

The profile of the packaged transducer is shown in Fig. 2(a). A 10 mm long, 1.6 mm diameter stainless steel tube was used as the transducer housing. A piezoelectric PZT piece with dimensions of $0.5\times0.5\times0.48$ mm^3 was mounted at the tip of the stainless steel tube as an active element. With a larger piece of ceramic disk, the longitudinal piezoelectric coefficient d_{33} was measured by using a piezoelectric meter (Model ZJ-3D, Institute of Acoustics, Academia Sinica) by direct measurement of the piezoelectric charge generated during the application of a uniaxial sinusoidal stress. A thin copper wire was glued to the bottom electrode of the PZT by using conductive silver epoxy as the hot line, and the upper

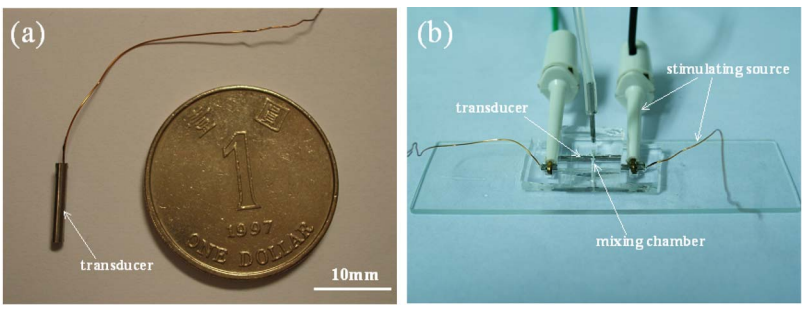

FIG. 2. (Color online) (a) Photograph of a packaged ultrasonic transducer with a coin for size reference and (b) photograph of the integrated device stimulated by external source.

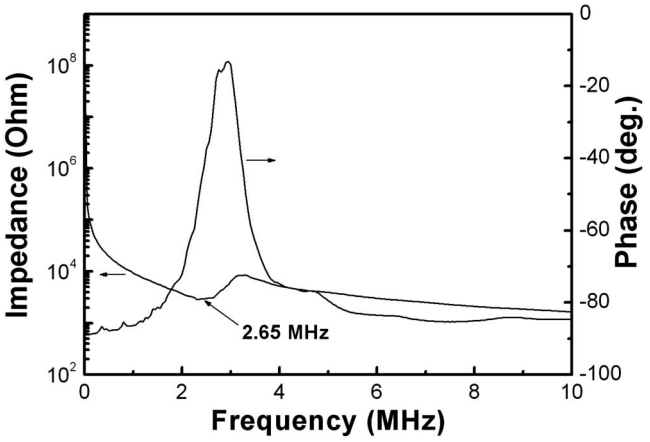

FIG. 3. (Color online) Impedance and phase spectrum dependence of the frequencies of one ultrasonic transducer.

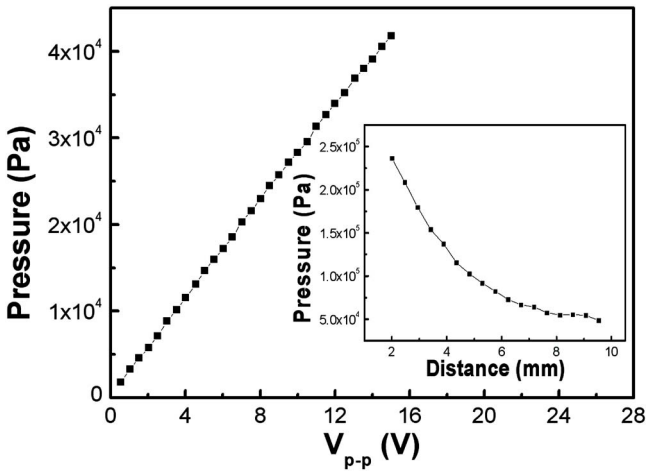

FIG. 4. (Color online) Pressure of BAWs of one ultrasonic transducer dependence of input voltage $V_{p\text{-}p}$ (peak to peak value). Inset: Pressure dependence of the distance between the transducer and hydrophone in the far field.

electrode surface was connected to the edge of connector as the ground terminal. After filling the epoxy resin backing, the front face of transducer was sealed with silicon rubber as a waterproof layer. Pressure measurement of the ultrasonic transducer was carried out in a water tank. A function generator (Model 8116A Pulse/Function Generator, HP) through a high frequency amplifier (Model 25A250, 25 W, 10 kHz–250 MHz, Amplifier Research) was used to excite the transducer. The acoustic waves were received by a standard polyvinylidene fluoride (PVDF) bilaminar shielded membrane hydrophone with an active element of diameter 0.5 mm (GEC-Marconi, Type Y-34-3598) together with a matched amplifier (NPL Amplifier Type 55641, $5\times$Gain). The voltage generated by the hydrophone was measured by using a digital oscilloscope (HP, Infinium oscilloscope, 500 MHz, 2 GSa/s). The transducer was placed at a distance in the far-field region of acoustic waves (distance $>a^2/\lambda$, where a is the transducer radius and λ is the wavelength of the acoustic wave).[21,22] In our case, $a^2/\lambda \approx 0.1$ mm when considering aqueous based solutions (speed of sound ≈ 1500 m/s) at 2.5 MHz, which is in the same scale when they are confined into the microfluidic channel (200 μm).

III. RESULTS AND DISCUSSION

A. Acoustic characteristics of ultrasonic transducers

Figure 3 shows the frequency spectrum of a single ultrasonic transducer that was obtained by using a precision impedance analyzer (Agilent 4294A, Agilent Technologies Corp.). It can be seen that the first resonance frequency is at 2.65 MHz, which corresponds to the thickness as well as the lateral mode resonances of the piezoelectric element as the thickness and lateral dimension of the element are close to 0.5 mm. The impedance mainly depends on the dimensions of the piezoelectric element and the geometric parameters of the transducer. Each transducer was precisely machined and adjusted to give a similar resonance frequency. Details can be found in Table I for seven ultrasonic transducers labeled from 1 to 7 in our work, among which 2 and 7 were chosen to be scaled in the microfluidic chamber as they have the same resonance frequency of 2.65 MHz.

Pressure calibration of the ultrasonic transducers was conducted in water at room temperature. Figure 4 shows the acoustic pressure dependence of the input voltage curve of the transducer measured by the PVDF membrane hydrophone in the far field with a sensitivity of 0.222 μV/Pa at 2.65 MHz. The results show that the pressure increases with the increase in input voltage $V_{p\text{-}p}$ (peak to peak value) and a good linear relationship is found. The maximum pressure can reach about 4.2×10^4 Pa with a voltage of 15 V. To better understand the induced pressure, the pressure dependence of distance between the transducer and hydrophone was illustrated in the inset of Fig. 4. The highest pressure can reach a value of 2.4×10^5 Pa at a distance of 2 mm, indicating a satisfactory acoustic performance for those ultrasonic transducers.

It should be noted here that this type of microfluidic device shows a remarkable characteristics of low energy consumption. The effective power consumption P_e can be approximated by the following:[23]

TABLE I. Effective power consumptions P_e of ultrasonic transducers at first resonance frequencies f_{first} when driven by an ac voltage with a peak-peak value of 10 V.

	1	2	3	4	5	6	7
d_{33} (pC/N)	455	550	500	495	530	560	540
f_{first} (MHz)	2.46	2.65	2.57	2.50	2.48	2.50	2.65
R_f (Ω)	2479.7	2834.3	2232.4	2495.4	1885.9	1609.2	2207.3
P_e (mW)	5.04	4.41	5.60	5.01	6.63	7.77	5.66

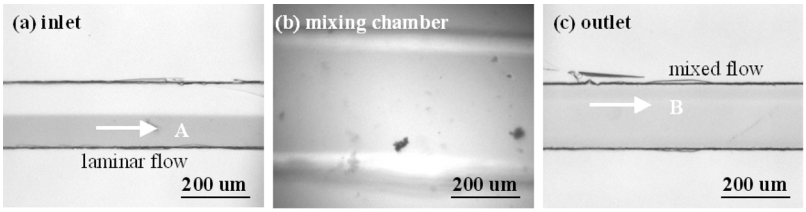

FIG. 5. (Color online) Laminar turbulence of oil phase in mixing chamber with (a) laminar flow of inlet, (b) turbulence in mixing chamber, and (c) mixed flow of outlet. The oil inlets were injected at a rate of 50 μL/h and the ultrasonic transducers were driven at 2.65 MHz with 10 $V_{p\text{-}p}$.

$$P_e = IV \approx \frac{V_e^2}{R_f} = \frac{1}{8}\frac{V_{p\text{-}p}^2}{R_f},$$

where V_e is the effective voltage on the ultrasonic transducer and R_f is the minimum impedance at the first resonance frequency. From Table I, it can be seen that the effective power consumption of the device is lower than 10 mW for all of the transducers, which makes a negligible Joule heating effect. Such a low consumption of energy is advantageous in many biological applications, especially in biological reagents, to increase the interfacial area and, consequently, to enhance the bioreaction with a high efficiency.

B. Fluid dynamic analyses and mixing efficiency of the active mixer

The Reynolds number (R_e) is the most important dimensionless number in fluid dynamics to determine whether a flow will be laminar or turbulent as follows:[24]

$$R_e = \frac{\rho v L}{\mu},$$

where v is the average velocity in the outlet channel, μ and ρ are the viscosity and density of pure water, respectively. L is the hydraulic diameter given by

$$L = \frac{4S}{W},$$

where S and W are the area and the wetted perimeter of the channel cross section, respectively.

In our case, a simplicity model is chosen with the same solution flows in the two inlets. The PDMS channel of top layer is 200 μm wide and 10 μm deep [Fig. 1(a)], and the mixing chamber is 1 mm wide, 2 mm deep, and 2 mm long [Fig. 1(b)]. In order to quantify the Reynolds number, considering a value for the outlet average velocity $v = 2 \times 10^{-3}$ m/s, the viscosity of pure water $\mu = 10^{-3}$ kg/(ms), and $\rho = 1000$ kg/m^3 at room temperature. The area and wetted perimeter of the top-layer PDMS channel cross section $S_1 = 2 \times 10^{-9}$ m^2, $W_1 = 4.2 \times 10^{-4}$ m, yields a Reynolds number $R_{e1} = 3.8 \times 10^{-2}$. This value indicates that the flow is indeed laminar, about five orders of magnitude below the transition point to turbulent flow ($R_e \approx 4000$). Similarly, the area and wetted perimeter of the mixing chamber cross section $S_2 = S_1 + S_2 \approx 2 \times 10^{-6}$ m^2, $W_2 \approx 6 \times 10^{-3}$ m, yields a Reynolds number $R_{e2} = 2.67$, which is also more than two orders of magnitude below the transition point to turbulent flow.

However, the laminar states will be dramatically changed when the streams with a limited volume flow from the PDMS channel of top layer into the mixing chamber due to the sharp descent along the microfluidic channel. Indeed, the velocity of fluid in PDMS channel will be shifted when entering into the mixing chamber, leading to a change in inertial forces (ρV). Considering the difference between the Reynolds numbers of PDMS channel and mixing chamber, the ratio $n = R_{e2}/R_{e1}$ is about 70, indicating related turbulent characters due to the unique structure of device. It is difficult to predict the exact ratio of the Reynolds numbers for which the flow is fully turbulent in the mixing chamber. However, the turbulent mixing will be largely enhanced if the ultrasonic transducers are actuated during the mixing process.

Figure 5 shows the turbulent mixing of two laminar oil streams flowing cross the mixing chamber at an injection rate of 50 μL/h. The oil phase in region A [Fig. 5(a)] of the microchannel was dyed by Sudan red (amethoxybenzenazo-β-naphthol, $C_{16}H_{12}N_2O$). By adjusting the flow rate, stable laminar flows were obtained. A turbulent mixing occurred in the mixing chamber and it became intensively strengthened with the ultrasonic energy [Fig. 5(b)]. A complete mixing was obtained in the outlet flow of region B [Fig. 5(c)], confirming a high mixing efficiency when the fluids flow across the mixing chamber combined with ultrasonic excitation.

The mixing efficiency α can be quantified for the mixed fluids as follows:[25,26]

$$\alpha = \left(1 - \frac{\int_0^h |C^+ - C_\infty^+| dy}{\int_0^h |C_i^+ - C_\infty^+| dy}\right) \times 100\%,$$

where C_∞^+ (=0.5) is the completely mixed condition on a normalized scale and C_i^+ (=0 or 1) is the initial unmixed states of two fluid streams, respectively. Two normalized scales are defined as $C^+ = C/C_0$, where C_0 is the initial concentration in the region A of Fig. 5(a) and C is the mixed concentration in the region B of Fig. 5(c), denoting the normalized concentration profile of streams across the channel width; $Y^+ = y/h$, where y is the linear variable value across the channel from top to bottom and h is the width of the channel, respectively. Figure 6 shows the mixing efficiency caused by different applied ac voltages at a frequency of 2.65 MHz for the active mixer. The concentration was calculated based on the median grayscale intensity in the images in the microchannels. The mixing efficiency in the center of a microchannel increases with the applied ac voltage and the maximum value was about 90% for 10 $V_{p\text{-}p}$, illustrating a relative high efficiency obtained in the integrated device (see Fig. 6). The measured parameters that may vary over time, such as lamp intensity and image median, drive the uncertainties in the channel and an average value is supposed to plot in the figure.

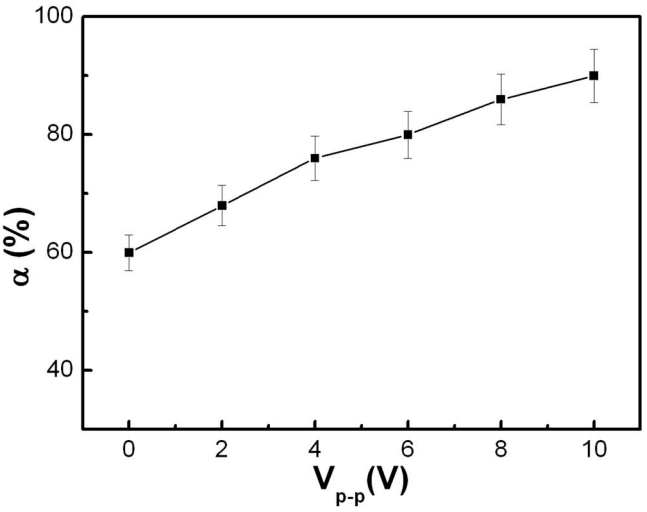

FIG. 6. (Color online) The mixing efficiency in the center of the microchannel at a frequency of 2.65 MHz for active mixers. The oil inlets were injected at a rate of 50 μL/h and the ultrasonic transducers were driven at 2.65 MHz.

Two additional test experiments have also been performed. The first one consists of observation of ultrasonic driven motion in Fe_3O_4 colloids of different sizes. At an injection rate of 5 μL/h and an ac voltage of 10 V_{p-p} at 2.65 MHz, we observed that the particles made a complete turn within a couple of second (not shown here). No obvious increase of temperature was found during the mixing due to low power consumption. In order to evaluate the possible tissue of damage during the acoustic mixing, yeast cells were grown with a continuously cell perfusion of cell culture media at a rate of 2 μL/h at 2.65 MHz. A clear proliferation effect has been observed after 2 h coloration (not shown here). This would indicate that no long-term effects resulted from the acoustic force on live cells. Therefore, it can be anticipated that the device can be employed to study proliferation of cells by using different functional media.

IV. CONCLUSIONS

We presented a simple method of active mixing based on BAWs with the help of a pair of small size ultrasonic transducers integrated into a microfluidic chamber. The mixing efficiency of laminar flows was analyzed by taking into account both microfluidic channel geometry and acoustic actuation. The integrated device enables flexible manipulation and has a low power consumption (<10 mW) without causing obvious Joule heat. Compared to other methods of active mixing based on acoustic wave, this configuration has the advantage of versatile mixing with a relative high mixing efficiency, although it needs further miniaturization. It is believed that such a device is capable not only of active mixing but also of precise particle handling, thereby providing a simple approach for fast prototyping of acoustic-wave-based microfluidic devices.

ACKNOWLEDGMENTS

This project was supported by the Centre for Smart Materials of the Hong Kong Polytechnic University. Financial support from PolyU internal Grant No. 1-ZV46 is acknowledged. This work was also partially supported by the Microfluidic Laboratory in Physics Department of Wuhan University.

[1] K. Hosokawa, T. Fujii, and I. Endo, Anal. Chem. **71**, 4781 (1999).
[2] H. H. Bau, J. Zhong, and M. Yi, Sens. Actuators B **79**, 207 (2001).
[3] M. Yi, S. Qian, and H. H. Bau, J. Fluid Mech. **468**, 153 (2002).
[4] P. K. Dasgupta, K. Surowiec, and J. Berg, Anal. Chem. **74**, 208A (2002).
[5] D. J. Harrison, K. Fluri, K. Seiler, Z. H. Fan, C. S. Effenhauser, and A. Manz, Science **261**, 895 (1993).
[6] H. P. Chou, C. Spence, A. Scherer, and S. Quake, Proc. Natl. Acad. Sci. U.S.A. **96**, 11 (1999).
[7] Y. Chen and A. Pépin, Electrophoresis **22**, 187 (2001).
[8] G. M. Whitesides, E. Ostuni, S. Takayama, and D. E. Ingber, Annu. Rev. Biomed. Eng. **3**, 335 (2001).
[9] A. O. El-Moctar, N. Aubry, and J. Batton, Lab Chip **3**, 273 (2003).
[10] P. Gravesen, J. Branebjerg, and O. S. Jensen, J. Micromech. Microeng. **3**, 168 (1993).
[11] W. K. Tseng, J. L. Lin, W. C. Sung, S. H. Chen, and G. B. Lee, J. Micromech. Microeng. **16**, 539 (2006).
[12] I. Glasgow and N. Aubry, Lab Chip **3**, 114 (2003).
[13] P. Paik, V. K. Pamula, M. G. Pollak, and R. B. Fair, Lab Chip **3**, 28 (2003).
[14] R. M. Moroney, R. M. White, and R. T. Howe, Appl. Phys. Lett. **59**, 774 (1991).
[15] W. Nyborg, *Physical Acoustics* (Academic, New York, 1965), Vol. II, Pt. B, Chap. 11.
[16] O. V. Rudenko, A. P. Sarvazyan, and S. Y. Emilianov, J. Acoust. Soc. Am. **99**, 2791 (1996).
[17] Z. Yang, S. Matsumoto, H. Goto, M. Matsumoto, and R. Maeda, Sens. Actuators, A **93**, 266 (2001).
[18] T. Laurell, F. Petersson, and A. Nilsson, Chem. Soc. Rev. **36**, 492 (2007).
[19] Z. Yang, H. Goto, M. Matsumoto, and R. Maeda, Electrophoresis **21**, 116 (2000).
[20] R. H. Liu, J. Yang, M. Z. Pindera, M. Athavale, and P. Grodzinski, Lab Chip **2**, 151 (2002).
[21] H. L. W. Chan, S. T. Lau, K. W. Kwok, Q. Q. Zhang, Q. F. Zhou, and C. L. Choy, Sens. Actuators, A **75**, 252 (1999).
[22] A. A. Doinikov, J. Acoust. Soc. Am. **101**, 713 (1997).
[23] D. A. Bradley, *Basic Electrical Power and Machines* (Chapman and Hall, London, 1994).
[24] D. Li, *Electrokinetics in Microfluidics* (Elsevier, New York, 2004).
[25] D. Erickson and D. Li, Langmuir **18**, 8949 (2002).
[26] D. Erickson and D. Li, Langmuir **18**, 1883 (2002).